The Antifouling and Fouling-Release Perfomance of Hyperbranched Fluoropolymer (HBFP)−Poly(ethylene glycol) (PEG) Composite Coatings Evaluated by Adsorption of Biomacromolecules and...

ARTICLE *in* LANGMUIR · APRIL 2005

Impact Factor: 4.46 · DOI: 10.1021/la048015o · Source: PubMed

The Antifouling and Fouling-Release Perfomance of Hyperbranched Fluoropolymer (HBFP)−Poly(ethylene glycol) (PEG) Composite Coatings Evaluated by Adsorption of Biomacromolecules and the Green Fouling Alga *Ulva*

Chakravarthy S. Gudipati,[†] John A. Finlay,[‡] James A. Callow,[‡] Maureen E. Callow,[‡] and Karen L. Wooley*,[†]

Centre for Materials Innovation and Department of Chemistry, Washington University, One Brookings Drive, Saint Louis, Missouri 63130-4899 and School of Biosciences, The University of Birmingham, Birmingham, B15 2TT, United Kingdom

Received August 5, 2004. In Final Form: January 3, 2005

Cross-linked hyperbranched fluoropolymer (HBFP) and poly(ethylene glycol) (PEG) amphiphilic networks with PEG weight percentages of 14% (HBFP−PEG14), 29% (HBFP−PEG29), 45% (HBFP−PEG45), and 55% (HBFP−PEG55) were prepared on 3-aminopropyl)triethoxysilane (3-APS) functionalized microscope glass slides for marine antifouling and fouling-release applications. The surface-free energies (γ_s), polar (γ_s^p and γ_s^{AB}), and dispersion (γ_s^d and γ_s^{LW}) components were evaluated using advancing contact angles by two-liquid geometric-mean and three-liquid Lifshitz−van der Waals acid−base approaches. The HBFP coating exhibited a low surface energy of 22 mJ/m^2, while the γ_s and γ_s^p of the cross-linked HBFP−PEG coatings increased proportionally with the PEG weight percentages in the networks. The adsorption of bovine serum albumin (BSA), lectin from *Codium fragile* (CFL), lipopolysaccharides from *Escherichia coli* (LPSE) and *Salmonella minnesota* (LPSS) upon glass, APS-glass, HBFP, PEG, and the cross-linked HBFP−PEG network coatings were investigated by fluorescence microscopy. The marine antifouling and fouling-release properties of the cross-linked HBFP−PEG coatings were evaluated by settlement and release assays involving zoospores of green fouling alga *Ulva* (syn. *Enteromorpha;* Hayden, H. S.; Blomster, J.; Maggs, C. A.; Silva, P. C.; Stanhope, M. J.; Waaland, J. R. *Eur. J. Phycol.* **2003**, *38*, 277). The growth and release of *Ulva* sporelings were also investigated upon the HBFP−PEG45 coating in comparison to a poly(dimethylsiloxane) elastomer (PDMSE) standard material. Of the heterogeneous cross-linked network coatings, the maximum resistances to protein, lipopolysaccharide, and *Ulva* zoospore adhesion, as well as the best zoospore and sporeling release properties, were recorded for the HBFP−PEG45 coating. This material also exhibited better performance than did a standard PDMSE coating, suggesting its unique applicability in fouling-resistance applications.

Introduction

Biofouling of underwater structures and ships' hulls in particular results in increased operational and maintenance costs.[1] Marine biofouling has been controlled traditionally through the use of antifouling paints that rely on the release of toxic ingredients such as cuprous oxide and organotin compounds. The latter are now proscribed and the former is under scrutiny because of environmental concerns; hence, novel environmentally benign solutions to control biofouling are being sought with urgency.[2,3] The primary mechanism in the attachment of marine organisms to surfaces involves secretion of protein or glycoprotein adhesives.[4−6] Therefore, it is of little surprise that significant attention has been directed toward development of efficient protein-resistant surfaces[7−11] for marine antifouling[12] as well as for other biomedical applications.[13,14] Even though the ability to resist protein and glycoprotein adsorption remains imperative for a coating to prevent marine fouling, it has been suggested that surface-free energy, mechanical properties, and wettability also play an important role in defining the extent to which a surface can resist biofouling and facilitate fouling release.[15−17] In this regard, the potency of fluoropolymers[12,18,19] and silicone elastomers,[20,21] which emerged as the most promising candidates, have been

* To whom correspondence should be sent. E-mail: klwooley@artsci.wustl.edu; tel: (314) 935-7136; fax # (314) 935-9844.

[†] Washington University.

[‡] The University of Birmingham.

(1) Townsin, R. L. *Biofouling* **2003**, *19*, 9.
(2) Callow, M. E. *Biodeterioration Abstr.* **1996**, *10*, 411.
(3) Swain, G. E. *Paint Coatings Europe*, July 1999, pp 18−25.
(4) Vreeland, V.; Waite, J. H.; Epstein, L. *J. Phycol.* **1998**, *34*, 1.
(5) Kamino, K.; Inoue, K.; Maruyama, T.; Takamatsu, N.; Harayama, S.; Shizuri, Y. *J. Biol. Chem.* **2000**, *275*, 27360.
(6) Stanley, M. S.; Callow, M. E.; Callow, J. A. *Planta* **1999**, *210*, 61.
(7) Ostuni, E.; Grzybowski, B. A.; Mrksich, M.; Roberts, C. S.; Whitesides, G. M. *Langmuir* **2003**, *19*, 1861.
(8) Hester, J. F.; Banerjee, P.; Won, Y. Y.; Akthakul, A.; Acar, M. H.; Mayes, A. M. *Macromolecules* **2002**, *35*, 7652.
(9) Groll, J.; Amiregoulova, E. V.; Ameringer, T.; Heyes, C. D.; Rocker, C.; Nienhaus, U.; Moller, M. *J. Am. Chem. Soc.* **2004**, *126*, 4234.
(10) Griesser, H. J.; Hartley, P. G.; McArthur, S. L.; McLean, K. M.; Meagher, L.; Thissen, H. *Smart Mater. Struct.* **2002**, *11*, 352.
(11) Bohringer, K. F. *J. Micromech. Microeng.* **2003**, *13*, S1.
(12) Youngblood, J. P.; Andruzzi, L.; Ober, C. K.; Hexamer, A.; Kramer, E. J.; Callow, J. A.; Finlay, J. A.; Callow, M. E. *Biofouling* **2003**, *19*, 91.
(13) Tosatti, S.; DePaul, S. M.; Askendal, A.; VandeVondele, S.; Hubbell, J. A.; Tengvall, P.; Textor, M. *Biomaterials* **2003**, *24*, 4949.
(14) Wagner, V. E.; Koberstein, J. T.; Bryers, J. D. *Biomaterials* **2004**, *25*, 2247.
(15) Finlay, J. A.; Callow, M. E.; Ista, L. K.; Lopez, G. P.; Callow, J. A. *Integr. Comput. Biol.* **2002**, *42*, 1116.
(16) Brady, R. F., Jr.; Singer, I. L. *Biofouling* **2000**, *16*, 1.
(17) Sigal, G. B.; Mrksich, M.; Whitesides, G. M. *J. Am. Chem. Soc.* **1998**, *120*, 3464.
(18) Pullin, R. A.; Nevell, T. G.; Tsibouklis, T. *Mater. Lett.* **1999**, *39*, 142.
(19) Brady, R. F., Jr.; Bonafede, S. J.; Schmidt, D. L. *Surf. Coat. Int.* **1999**, *82*, 582.
(20) Berglin, M.; Wynne, K. J.; Gatenholm, P. *J. Colloid Interface Sci.* **2003**, *257*, 383.
(21) Bullock, S.; Johnston, E. E.; Willson, T.; Gatenholm, P.; Wynne, K. J. *J. Colloid Interface Sci.* **1999**, *210*, 18.

10.1021/la048015o CCC: $30.25
Published on Web 00/00/0000 PAGE EST: 9.7

explained in terms of their low surface energy and interesting mechanical properties.[16,22] Fouling-release coatings based on silicone elastomers are commercial products that "release" accumulated biofouling either by the hydrodynamic forces generated as a vessel moves through the water or by cleaning and have been researched widely.[23−25] However, the present generation of fouling-release coatings has several disadvantages and is unsuitable for use on the majority of vessels.[3] The variety of fouling organisms and environmental conditions worldwide makes the task of developing a coating that resists fouling and self-cleans very challenging, and novel nontoxic solutions are urgently needed.

Cross-linked hyperbranched fluoropolymer (HBFP)−poly(ethylene glycol) (PEG) amphiphilic network coatings are designed to prevent biofouling in general and marine fouling in particular by providing surfaces with compositional and topographical complexities that are expected to discourage any favorable interactions with the adhesive biomacromolecular segments secreted by a particular marine organism. Our strategy is based on the hypothesis that if the surface presents optimal nanoscale heterogeneity in terms of composition, morphology, and topography, it becomes energetically unfavorable for the protein or glycoprotein "glue" to adhere via either hydrophobic or hydrophilic interactions, thereby weakening the interactions of the organism itself, with the surface. While earlier work focused on fundamental surface characteristics, such as composition, topography, and morphology, of the HBFP−PEG coatings,[26] this present study emphasizes the correlation between their resistance to biofouling and the surface energetics, in conjunction with the previous observations. It has been established already that coatings of cross-linked HBFP−PEG networks exhibit complex morphologies and topographies originating because of the characteristic phase segregation of the HBFP and PEG domains.[27] Each of the surface properties, such as composition, topography, and wettability, depended on the extent of phase separation, which was dependent on the relative composition of PEG/HBFP. Having demonstrated that nanoscale and microscale morphological and topographical heterogeneities can be achieved by varying the coating thickness[27] as well as the relative composition of PEG as 14, 29, 45, and 55 wt %, investigation of the influence of these factors and the surface energies upon the antibiofouling characteristics of the HBFP−PEG coatings was undertaken. In this study, the surface-free energies, together with the polar and dispersion components of HBFP, and the cross-linked HBFP−PEG coatings were calculated from the advancing contact angles of water (WT), diiodomethane (DM), and ethylene glycol (EG) using geometric-mean and Lifshitz−van der Waals-acid−base models. The resistance of the cross-linked HBFP−PEG network coatings toward protein and lipopolysaccharide adsorption were investigated by employing bovine serum albumin (BSA), a lectin protein from *Codium fragile* (CFL), and lipolysaccharides from *Escherichia coli* and *Salmonella minnesota* (LPSE and LPSS, respectively) as model systems to obtain a holistic understanding of the antifouling behavior of the coatings toward hydrophobic and amphiphilic biomacromolecules. With respect to the specific practical application of the HBFP−PEG coatings to prevent *marine biofouling*, laboratory assays were conducted employing zoospores of the green alga *Ulva*,[28] which is the most widespread alga that fouls man-made structures including ships and submarines. Colonization of substrata by the *Ulva* occurs through the production of motile zoopores, which locate a suitable surface on which to settle.[29] Permanent adhesion is achieved through the rapid secretion of glycoprotein adhesive that permanently anchors the spore to the substratum.[6,30] The adhered spores rapidly germinate forming sporelings that eventually grow into mature plants.

Experimental Section

Materials. Diisopropylethylamine (DIEA), 3-aminopropyltriethoxysilane (3-APS), bis(3-aminopropyl) terminated poly(ethylene glycol) (PEG) ($M_n = 1600$ Da, $DP_n = 34$), and all solvents were purchased from Aldrich Chemical Co. Chloroform and methanol were used as purchased. Tetrahydrofuran (THF) was distilled from Na. For the contact angle experiments, DI-water was obtained from a Barnstead NANOpure system (18.0 MΩ-cm), and diiodomethane (99.0%) and ethylene glycol (99.8%) were used as purchased from Aldrich Chemical Co. The monoglycidyl ether of PEG ($M_n = 3400$ Da, $DP_n = 78$) was purchased from Scientific Polymer Products. The hyperbranched fluoropolymer (HBFP) (**1**) was synthesized according to the procedure previously reported.[31] HBFP (**1a**, $M_n = 9700$, $DP_n = 20$, $M_w/M_n = 1.8$) was used in the preparation of the cross-linked HBFP−PEG coatings for contact angle measurements, HBFP (**1b**, $M_n = 7900$, $DP_n = 16$, $M_w/M_n = 2.2$) was used in the preparation of materials for fluorescence microscopy experiments, and HBFP (**1c**, $M_n = 9400$ Da, $DP_n = 20$, $M_w/M_n = 2.2$) was used in the HBFP−PEG coatings for *Ulva* zoospore attachment and release studies.

General Procedure for the Preparation of Hyperbranched Fluoropolymer Cross-Linked with Bis(3-aminopropyl) Terminated Poly(ethylene glycol). Cross-linked HBFP−PEG networks with PEG weight percentages of 14 wt % (HBFP−PEG14), 29 wt % (HBFP−PEG29), 45 wt % (HBFP−PEG45), and 55 wt % (HBFP−PEG55) were prepared according to the procedure previously reported as method II.[26,27]

General Procedure for the Preparation of Coatings on Microscope Glass Slides. For contact angle measurements, microscope glass slides (Fisher Scientific, $75 \times 25 \times 1$ mm^3) were flame cleaned for 15 s, immersed in a HCl (13 M):methanol mixture for 2 h and then in HCl (13 M) solution for 2 h, followed by thorough rinsing with DI water (Barnstead NANOpure system, 18.0 MΩ-cm). The slides were then dried under vacuum at 50 °C for 4 h. The glass slides were then immersed in a 5% (v/v) solution of 3-aminopropyltriethoxysilane (3-APS) in anhydrous toluene for 6 h at room temperature, followed by curing at 190 °C under vacuum for 12 h, to allow for the functionalization.[32] For the fluorescence microscopy measurements, and the *Ulva* zoospore attachment and release assays, the microscope glass slides were cleaned in a $CHCl_3$:methanol (50:50) solvent mixture in an ultrasonic cleaner for 30 min and dried under vacuum at room temperature in a desiccator for 1 h. The slides were typically stored under nitrogen for 30 min, and then 3-aminopropyltriethoxysilane (3-APS) (200 μL) was introduced to allow for functionalization by vapor deposition at room temperature, under nitrogen for 2 h, according to the procedure

(22) Shafrin, E. G.; Zisman, W. A. *J. Phys. Chem.* **1960**, *64*, 519.
(23) Swain, G. W.; Schultz, M. P. *Biofouling* **1996**, *10*, 187.
(24) Stein, J.; Truby, K.; Darkangelo-Wood, C.; Stein, J.; Gardner, M.; Swain, G.; Kavanagh, C.; Kovach, B.; Schultz, M.; Wiebe, D.; Holm, E.; Montemarano, J.; Wendt, D.; Smith, C.; Meyer, A. *Biofouling* **2003**, *19*, 71.
(25) Stein, J.; Truby, K.; Darkangelo-Wood, C.; Takemori, M.; Vallance, M.; Swain, G.; Kavanagh, C.; Kovach, B.; Schultz, M.; Wiebe, D.; Holm, E.; Montemarano, J.; Wendt, D.; Smith, C.; Meyer, A. *Biofouling* **2003**, *19*, 87.
(26) Gudipati, C. S.; Greenlief, C. M.; Johnson, J. A.; Pornpimol, P.; Wooley, K. L. *J. Polym. Sci., Part A: Polym. Chem.* **2004**, *42*, 6179.
(27) Gan, D.; Mueller, A.; Wooley, K. L. *J. Polym. Sci., Part A: Polym. Chem.* **2003**, *41*, 3531.
(28) Hayden, H. S.; Blomster, J.; Maggs, C. A.; Silva, P. C.; Stanhope, M. J.; Waaland, J. R. *Eur. J. Phycol.* **2003**, *38*, 277.
(29) Callow, M. E.; Callow, J. A. *Biofouling* **2000**, *15*, 49.
(30) Callow, J. A.; Stanley, M. S.; Wetherbee, R.; Callow, M. E. *Biofouling* **2000**, *16*, 141.
(31) Mueller, A.; Kowalewski, T.; Wooley, K. L. *Macromolecules* **1998**, *31*, 776.
(32) Emoto, K.; Van Alstine, J. M.; Harris, J. M. *Langmuir* **1998**, *14*, 2722.

reported in the literature.[33] The slides were then coated by multiple cycles of immersion into a THF solution containing DIEA, HBFP, and PEG-$(NH_2)_2$ or into a solution of HBFP in THF (5% w/v) with intermediate drying. The glass slides were then heated at 100 °C for 1 h, under nitrogen. The PEG-grafted glass surfaces were prepared by the immersion of the 3-APS functionalized glass substrates in 10% (w/v) solution of monoglycidyl ether of PEG ($M_n = 3000$) in sodium phosphate buffer (0.05 M NaH_2PO_4−Na_2HPO_4, 0.15 M NaCl, pH 7.3) for 6 h at 60 °C.[32] For the *Ulva* spore and sporeling assays, all coated slides were equilibrated in sterile seawater for 24 h prior to the start of the bioassays. Acid-washed glass slides were incubated as standards. For comparative purposes, a foul-release poly(dimethylsiloxane) elastomer (PDMSE), T2 Silastic (Dow Corning), was included in the sporeling experiment. The details of preparation of T2 coated slides have been reported elsewhere.[34]

Contact Angle and Surface-Free Energy Measurements. Contact angle analysis upon the HBFP and the cross-linked HBFP−PEG network coatings was performed by the sessile drop technique using a Tantec CAM-microcontact angle meter equipped with a microsyringe and a flat-tipped needle. Advancing and receding contact angles of water (WT), diiodomethane (DM), and ethylene glycol (EG) were measured at room temperature, by initially placing a drop of the test liquid (2 μL) and increasing or decreasing the drop size by 1 μL, respectively, at a nominal rate of 0.5 μL/s, until the three-phase boundary line moved. The contact angles were measured within 15 s of addition or withdrawal of the test liquid from the original drop. Utmost care was taken to prevent vibrations that might distort the drop size during measurements. The reported values are an average of five such measurements on different regions of the same sample.

The polar (γ_s^p) and dispersion (γ_s^d) components of surface-free energies of the HBFP, and the cross-linked HBFP−PEG coatings, were calculated using Owens and Wendt's[35] two-liquid geometric-mean (eq 1)[36]

$$\gamma_{lv}(1 + \cos\theta) = 2\sqrt{\gamma_s^d \gamma_{lv}^d} + 2\sqrt{\gamma_s^p \gamma_{lv}^p} \quad (1)$$

$$\gamma_s = \gamma_s^p + \gamma_s^d \quad (2)$$

where γ_{lv}, γ_{lv}^p, and γ_{lv}^d are the total surface tension, polar, and dispersion components of the test liquids, respectively. The total surface-free energies of the coatings were computed as the sum of the γ_s^p and γ_s^d terms (eq 2).

The Lewis acid (γ_s^+) and Lewis base (γ_s^-) parameters of the surface energies were calculated using van Oss, Good, and Chaudhury's three-liquid Lifshitz−van der Waals acid−base model,[37,38] given by eqs 3−5

$$\gamma_{lv}(1 + \cos\theta) = 2\sqrt{\gamma_s^{LW}\gamma_{lv}^{LW}} + 2\sqrt{\gamma_s^+\gamma_{lv}^-} + 2\sqrt{\gamma_s^-\gamma_{lv}^+} \quad (3)$$

$$\gamma_s^{AB} = 2\sqrt{\gamma_s^+\gamma_s^-} \quad (4)$$

$$\gamma_s = \gamma_s^{LW} + \gamma_s^{AB} \quad (5)$$

where γ, γ^{LW}, and γ^{AB} are the total surface energy, Lifshitz−van der Waals (nonpolar), and acid−base (polar) components, respectively. The subscripts "s" and "lv" refer to the surface and the test liquid, respectively.

Adsorption of Biomacromolecules. The adhesion of various biological macromolecules conjugated with Alexa Fluor 488 (AF) dye was studied by fluorescence microscopy using an Olympus IX70 optical microscope fitted with a mercury medium-pressure arc lamp and an Olympus SC35 camera. The images were collected through a 10× objective. A filter cube with an excitation maximum of 470 ± 20 nm (band-pass) and an emission maximum of 500 nm (long pass) was used in these experiments. Alexa Fluor 488 (AF) dye conjugates of bovine serum albumin (BSA, mw 66 000 Da), lipopolysaccharides from *Salmonella minnesota* (LPSS, mw 3000 Da), and *E. coli* (LPSE, mw 10 000 Da) were purchased from Molecular Probes, Inc. The lectin from *Codium fragile* (CFL, mw 60 000 Da) was purchased from Sigma Chemical Company. The CFL was conjugated with AF by using an Alexa Fluor 488 Protein Labeling Kit (A-10235, Molecular Probes, Inc.), followed by elution through a Bio-Rad Bio-Gel P-30 fine size exclusion purification resin (Molecular Probes) to separate the free dye from the CFL-AF conjugate.

Each of the four AF-conjugated systems, bovine serum albumin (BSA), CFL, and lipopolysaccharides from *E. coli* (LPSE) and *Salmonella minnesota* (LPSS), was dissolved in phosphate-buffered saline (PBS) solution (pH 7.0) at a nominal concentration of 0.1 mg/mL, purified by dialysis (Slide-A-Lyzer tubing, 10 000 MWCO) against PBS buffer for 1 day in the dark, and then deposited (∼0.5 mL) onto the coatings and equilibrated for 10 min in the dark, at ambient temperature. The surfaces were then rinsed thoroughly with PBS buffer and allowed to dry for 10 min in the dark before the fluorescence microscopy images were captured. The fluorescence microscopy images were analyzed by "line profiling" using ImageJ software (NIH freeware, http://rsb.info.nih.gov/ij/), whereby the background from the fluorescence histograms were determined by visual inspection of the images and the pixel values above the background values were considered as emission from the surface. The fraction of the surface fluorescing (pixel count above the background value divided by the total pixel count) is reported as % fluorescence. A 100% fluorescence implies that the surface is totally green and 0% indicates that the surface is totally dark. The dye/protein ratios were calculated as 0.8 and 1.3 for the BSA−AF and CFL−AF conjugates, respectively, from the measured UV absorbance of the Alexa Fluor dye at 490 nm using a molar extinction coefficient of 71 000 cm^{-1} M^{-1}. Since the dye/protein ratio is ∼1, it is assumed that the fluorescence emission intensity is directly proportional to the amount of protein adsorbed on the surface. The histograms of intensity versus normalized pixel counts were obtained using image analysis tools in the MATLAB software.

Algal Assays. Zoospore Settlement and Removal. Fertile plants of *Ulva linza* were collected from Wembury Beach, England (latitude 50°18′ N; 4°02′ W). Zoospores were released and prepared for attachment experiments as described previously.[39] Ten-milliliter aliquots (1.5×10^6 spore mL^{-1}) were pipetted into individual compartments of polystyrene culture dishes (Fisher), each containing a glass microscope slide. Six replicates of each treatment were prepared. The dishes were incubated in the dark for 1 h before the slides were washed by passing backward and forward 10 times through a beaker of seawater to remove unattached spores. Three replicate slides of each treatment were fixed in 2.5% glutaraldehyde in seawater and processed as described in Callow et al.[39] Adhered spores were visualized by autofluorescence of chlorophyll and quantified by image analysis.[40] Thirty counts were taken at 1-mm intervals along the middle of the long axis of each of the three replicate slides. Means (n = 90) and 95% confidence limits were calculated and expressed as mean number of adhered spores/mm^2. The remaining three replicates were used to evaluate the strength of zoospore attachment. Slides were placed in a flow apparatus[41] that had been modified by fitting a higher capacity pump as described in Finlay et al.[15] Slides were exposed to a fully developed turbulent flow for 5 min at 55 Pa wall shear stress. The mean number of spores remaining attached to the surface after exposure to turbulent flow was compared with the mean number before the slides were subjected to flow. Data are expressed as percentage removal; 95% confidence limits were calculated from arcsine-transformed data.

(33) Lyubchenko, Y. L.; Gall, A. A.; Shlyakhtenko, L. S. *Methods Mol. Biol.* **2001**, *148*, 569.
(34) Callow, M. E.; Jennings, A. R.; Brennan, A. B.; Seegert, C. E.; Gibson, A.; Wilson, L.; Feinberg, A.; Baney, R.; Callow, J. A. *Biofouling* **2002**, *18*, 237.
(35) Owens, D. K.; Wendt, R. C. *J. Appl. Polym. Sci.* **1969**, *13*, 1741.
(36) Wu, S. *J. Polym. Sci., Polym. Symp.* **1971**, *34*, 19.
(37) van Oss, C. J.; Good, R. J.; Chaudhury, M. K. *J. Colloid Interface Sci.* **1986**, *111*, 378.
(38) van Oss, C. J.; Good, R. J.; Chaudhury, M. K. *Langmuir* **1988**, *4*, 884.
(39) Callow, M. E.; Callow, J. A.; Pickett-Heaps, J.; Wetherbee, R. *J. Phycol.* **1997**, *33*, 938.
(40) Callow, J. A.; Osborne, M. P.; Callow, M. E.; Baker, F.; Donald, A. M. *Biocolloids Surf., Part B: Interfaces* **2002**, *27*, 315.
(41) Schultz, M. P.; Finlay, J. A.; Callow, M. E.; Callow, J. A. *Biofouling* **2000**, *15*, 243.

Sporeling Growth and Attachment. The fouling-release properties of the most promising test surface (HBFP−PEG45) were compared with a Pt-cured poly(dimethylsiloxane) elastomer (PDMSE) standard using *Ulva* sporelings (young plants). Silastic T-2 (Dow-Corning Corporation) was applied to glass slides as described in Hoipkemeier-Wilson et al.[42] The modulus of the T2 PDMSE is 1.4 MPa, the water contact angle is typically 109 ± 3.5°, and the calculated surface energy is 23.0 ± 0.4 mN m^{-2}.[43] Acid-washed glass and cross-linked HBFP−PEG45 coated slides (four replicates of each) were exposed to a suspension of zoospores for 1 h as described above, at a density of 1×10^6 mL^{-1}. After washing, 10 mL of growth medium[44] was added to each dish compartment. The dishes were incubated at 20 °C with a 16 h:8 h light/dark cycle. The medium was changed every 2 days. After 8 days, sporelings were harvested by scraping with a razor blade from half of each slide. Biomass was determined by extraction of chlorophyll.[45] The mean amount of chlorophyll *a* (μg) cm^{-2} ± standard error is plotted.

To evaluate the strength of attachment of the sporelings, the slides were placed in the flow apparatus and exposed to turbulent flow as described above. The slides were positioned such that the area from which the biomass had been removed was at the leading edge with respect to water flow. Biomass was harvested from the remaining half of each slide. Percentage removal was calculated as for the spores. Bars represent the standard error of the mean from arcsine-transformed data.

Results and Discussion

Synthesis and Coating Preparation. The cross-linked networks of HBFP and diamine-terminated poly(ethylene glycol) (PEG) were prepared with the PEG weight percentages of 14% (HBFP−PEG14), 29% (HBFP−PEG29), 45% (HBFP−PEG45), and 55% (HBFP−PEG55), according to the previously established procedures.[26,27] Glass microscope slides, functionalized with 3-aminopropyltriethoxysilane (3-APS), were used as substrates for preparing the coatings of HBFP, diamine-terminated PEG, and the cross-linked HBFP−PEG networks (Scheme 1). This procedure allows for the covalent attachment of the polymeric network to the substrate, resulting in stable coatings that do not delaminate upon storage in water. The HBFPs from three different batches of slightly different molecular weights, **1a**, **1b**, and **1c**, were used in the current study, simply because of availability. There were no apparent differences in the network materials resulting from these three different precursors.

The coatings of cross-linked HBFP−PEG networks exhibit complex topographies and morphologies resulting from the phase segregation of the HBFP and PEG domains, as observed by atomic force microscopy and differential scanning calorimetry.[26,27] In these studies, the dimensions of the phase-separated domains were dependent on the relative composition of PEG/HBFP in the network. The surface composition of the cross-linked HBFP−PEG coatings was observed to be comprised of HBFP and PEG domains, and the surface concentration of the PEG segment increased in accordance with the bulk composition, as demonstrated by way of X-ray photoelectron spectroscopy measurements. Furthermore, the surfaces underwent reorganization upon contact with water, resulting in phase inversion because of the enhanced segregation of the PEG phase to the polymer−water interface.

Scheme 1. Covalent Attachment of the (a) HBFP, (b) PEG, and (c) HBFP−PEG Cross-Linked Networks to the 3-APS Functionalized Glass Microscope Slides

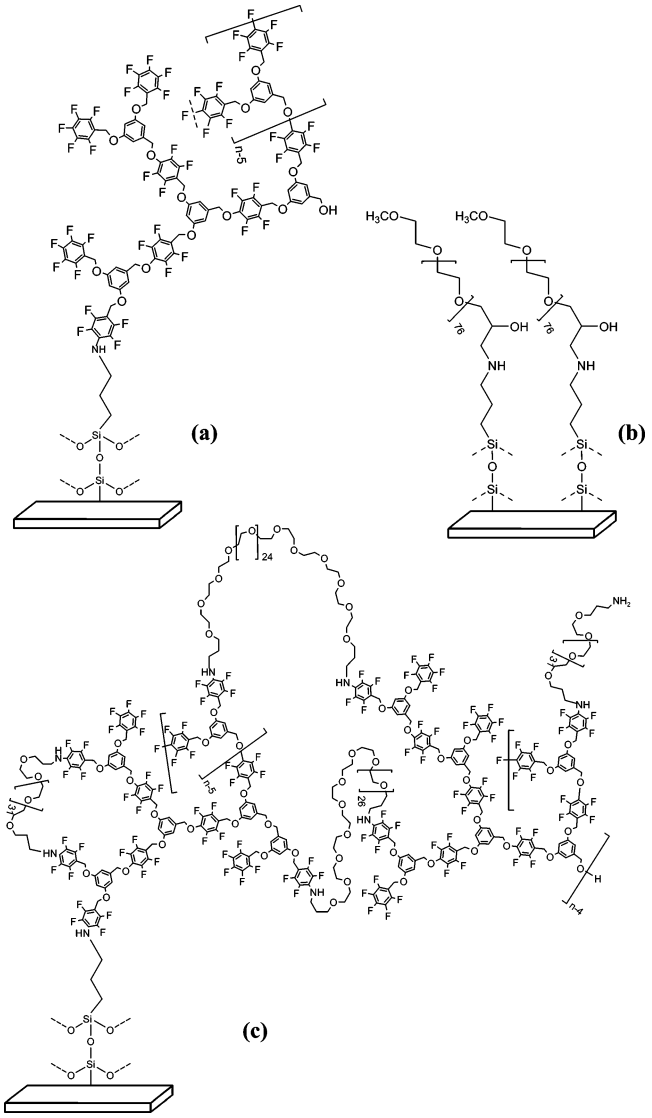

Contact Angle Measurements and Surface-Free Energy Calculations. Contact Angles and Contact Angle Hysteresis. The advancing and receding contact angles, summarized in Table 1, upon HBFP and the cross-linked HBFP−PEG coatings were determined by the sessile drop technique using water (WT), diiodomethane (DM), and ethylene glycol (EG) as test liquids having varying polarities. The advancing contact angle (θ_a) of water on HBFP was 109.2° ± 1.8° indicating its highly hydrophobic nature, while in comparison, each of the cross-linked HBFP−PEG network coatings exhibited lower contact angles of water in a decreasing trend with increase in the hydrophilic PEG composition in the HBFP−PEG networks. These observations are in agreement with the static contact angle measurements previously reported for the thin films of HBFP−PEG cross-linked networks.[26,27] Similar trends were also observed in the advancing contact angles of diiodomethane and ethylene glycol, indicating an increase in the surface energy of each of the HBFP−PEG coatings with increase in the PEG weight percentage. The receding contact angles (θ_r), summarized in Table 1, reflect significant hystereses ($\theta_a - \theta_r$) upon all of the cross-

(42) Hoipkemeier-Wilson, L.; Schumacher, J. F.; Carman, M. L.; Gibson, A. L.; Feinberg, A. W.; Callow, M. E.; Finlay, J. A.; Callow, J. A.; Brennan, A. B. *Biofouling* **2004**, *20*, 53.

(43) Feinberg, A. W.; Gibson, A. L.; Wilkerson, W. R.; Seegert, C. A.; Wilson, L. H.; Zhao, L. C.; Baney, R. H.; Callow, J. A.; Callow, M. E.; Brennan, B. A. *Synthesis and Properties of Silicones and Silicone-modified Materials*; Clarson, S. J., Fitzgerald, J. J., Owen, M. J., Smith, S. D., van Dyke, M. E., Eds.; ACS Symposium Series 838; American Chemical Society: Washington, DC, 2003; pp 196−211.

(44) Starr, R. C.; Zeikus, J. A. *J. Phycol.* **1987**, *23*, 1.

(45) Jeffrey, S. W.; Humphrey, G. F. *Biochem. Physiol. Pflanz.* **1975**, *167*, 191.

Table 1. Advancing (θ_a) and Receding (θ_r) Contact Angles of Water (WT), Diiodomethane (DM), and Ethylene Glycol (EG) upon Coatings of the Cross-Linked HBFP–PEG Networks, Measured by Sessile Drop Method[a]

	WT		DM		EG	
coating	θ_a	θ_r	θ_a	θ_r	θ_a	θ_r
HBFP	109.2 ± 1.8	98.0 ± 1.4	71.6 ± 1.7	63.6 ± 1.7	81.2 ± 1.8	72.0 ± 3.7
HBFP–PEG14	100.8 ± 2.3	76.4 ± 1.7	70.0 ± 1.4	61.6 ± 2.6	77.6 ± 1.7	59.2 ± 5.9
HBFP–PEG29	92.8 ± 1.1	67.2 ± 2.7	66.8 ± 1.1	57.2 ± 3.0	66.4 ± 0.9	47.6 ± 5.2
HBFP–PEG45	80.4 ± 3.3	50.0 ± 4.5	61.2 ± 1.1	46.8 ± 3.0	56.8 ± 1.1	37.2 ± 4.8
HBFP–PEG55	73.6 ± 2.2	48.4 ± 7.9	56.0 ± 0.0	40.8 ± 1.1	47.6 ± 0.9	30.0 ± 2.4

[a] HBFP (**1a**) was used in the preparation of the cross-linked HBFP–PEG materials for contact angle experiments.

linked HBFP–PEG network coatings, which are believed to result mainly from the heterogeneity in the surface-composition and also from to the effects of surface roughness. The water contact angle hystereses were 11.0 ± 1.0, 24.0 ± 2.0, 26.0 ± 2.0, 30.0 ± 6.0, and 25.0 ± 10.0 for the surfaces with PEG wt % of 0, 14, 29, 45, and 55%, respectively.

The observations are in agreement with several explanations in the literature regarding contact angle hysteresis, which was presumed to be occurring not only because of surface roughness or heterogeneity[46–48] but also because of other factors such as polymer dissolution, surface restructuring,[49] and solvent penetration.[50] In particular, the HBFP–PEG surfaces have already been shown to undergo reorganization because of swelling in the presence of water.[26] Similar surface reconstruction cannot be ruled out during the contact angle measurement using ethylene glycol as the test liquid. Therefore, it is possible that the large hystereses and significant scattering in the data (Table 1) obtained for the HBFP–PEG surfaces may have partially resulted from the swelling and reorganization of the PEG domains. Interestingly, Schmidt et al. have recently reported that coatings prepared by cross-linking a copolymer of heptadecafluorodecyl acrylate and acrylic acid with a copolymer of poly(2-isopropenyl-2-oxazoline) and methyl methacrylate exhibited lower contact angle hysteresis because of reduced solvent permeability, as well as better marine foulant-release properties.[50]

Surface-Free Energies. The total surface energies along with the polar and dispersive components for HBFP and the cross-linked HBFP–PEG network coatings were evaluated using advancing contact angles by geometric-mean (GM, eq 1)[35] and Lifshitz–van der Waals acid–base (LW-AB, eq 3)[37,38] approaches, all of which rely on Fowkes' model that assumes the total surface energy to be the sum of different interaction components (van der Waals dispersive, dipole, hydrogen bonding, etc.) at the solid–liquid interface. In the GM model, by measuring the contact angles of at least two liquids, one polar and one apolar, whose γ_{lv}^p and γ_{lv}^d values are known, two equations can be obtained from which the two unknowns γ_s^p and γ_s^d can be calculated. On the other hand, the LW-AB approach further resolves the polar contributions into Lewis acid (γ_s^+) and Lewis base (γ_s^-) parameters, while redefining γ_s^d as the Lifshitz–van der Waals parameter, γ_s^{LW}. In this approach, the contact angle values measured using at least three test liquids, two polar and one apolar, whose γ_{lv}^{LW}, γ_{lv}^+, and γ_{lv}^- values are known, are substituted into eq 3 to obtain three equations that can be solved for the three unknowns γ_s^{LW}, γ_s^+, and γ_s^-. In this study, water and ethylene glycol were chosen as the polar liquids and diiodomethane was used as the apolar liquid.

Table 2. The Polar (γ_{lv}^p), Dispersion (γ_{lv}^d), van Der Waals (γ_{lv}^{LW}), Electron-Donor (γ_{lv}^-), and Electron-Acceptor (γ_{lv}^+) Components of the Test Liquid Surface Tensions[a]

test liquid	γ_{lv} (mJ/m^2)	γ_{lv}^d (mJ/m^2)	γ_{lv}^p (mJ/m^2)	γ_{lv}^{LW} (mJ/m^2)	γ_{lv}^{AB} (mJ/m^2)	γ_{lv}^+ (mJ/m^2)	γ_{lv}^- (mJ/m^2)
WT	72.8	21.8	51.0	21.8	51.0	25.5	25.5
DM	50.8	48.5	2.3	50.8	0.0	0.0	0.0
EG	48.2	29.3	18.9	29.0	19.0	3.0	30.1

[a] Water (WT), and ethylene glycol (EG) were chosen as the polar liquids, while diiodomethane (DM) was used as the apolar liquid.[46,51–53]

Table 3. The Surface-Free Energies (γ_s) and Their Polar (γ_s^p) and Dispersion (γ_s^d) Components of HBFP and the Cross-Linked HBFP–PEG Coatings Calculated by the Two-Liquid Geometric-Mean (GM) Model[a]

coating	liquid pair	γ_s^p (mJ/ m^2)	γ_s^d (mJ/ m^2)	γ_s (mJ/m^2)
HBFP	DM–WT	0.10	22.36	22.46
	DM–EG	0.50	21.57	22.07
mean		0.30	21.97	22.27
HBFP–PEG14	DM–WT	1.21	21.67	22.88
	DM–EG	0.83	22.06	22.89
mean		1.02	21.90	22.92
HBFP–PEG29	DM–WT	2.97	22.17	25.14
	DM–EG	3.92	21.65	25.57
mean		3.45	21.91	25.36
HBFP–PEG45	DM–WT	6.60	23.47	30.07
	DM–EG	6.44	23.54	29.98
mean		6.52	23.51	30.03
HBFP–PEG55	DM–WT	10.80	24.71	35.52
	DM–EG	9.12	25.29	34.41
mean		9.96	25.00	34.96

[a] Diiodomethane (DM) was selected as the apolar liquid, while water (WT) and ethylene glycol (EG) were chosen as the polar liquids.

The polar (γ_{lv}^p), dispersion (γ_{lv}^d), Lifshitz–van der Waals (γ_{lv}^{LW}), acid–base (γ_{lv}^{AB}), electron-donor (γ_{lv}^-), and electron-acceptor (γ_{lv}^+) components for the test liquids are given in Table 2.[46,51–53] The total surface energy γ_s, the components (γ_s^p and γ_s^d) of the HBFP, and the cross-linked HBFP–PEG coatings calculated by the two-liquid GM model are summarized in Table 3.

The total surface energy of the HBFP coating was 22.27 mJ/m^2. The total surface energies of the cross-linked HBFP–PEG coatings increased as the PEG weight percent was varied as 14, 29, 45, and 55% (Table 3), because of the proportional augmented segregation of the high-energy PEG at the polymer–liquid interface. Similar behavior

(46) Wu, S. *Polymer Interface and Adhesion*; Marcel Dekker: New York, 1982.
(47) Kwok, D. Y.; Neumann, W. A. *Contact Angle, Wettability Adhes.* **2003**, *3*, 117.
(48) Extrand, C. W. *J. Colloid Interface Sci.* **1998**, *207*, 11.
(49) Chatelier, R. C.; Xie, X.; Gengenbach, T. R.; Griesser, H. J. *Langmuir* **1995**, *11*, 2576.
(50) Schmidt, D. A.; Brady, R. F., Jr.; Lam, K.; Schmidt, D. C.; Chaudhury, M. K. *Langmuir* **2004**, *20*, 2830.
(51) Balkenende, A. R.; Boogaard, V.; Scholten, M.; Willard, N. P.; Scholten, M.; Willard, N. P. *Langmuir* **1998**, *14*, 5907.
(52) Ho, C. C.; Khew, M. C. *Langmuir* **2000**, *16*, 1407.
(53) Turunen, M. P. K.; Laurila, T.; Kivilahti, J. K. *J. Polym. Sci., Part B: Polym. Phys.* **2002**, *40*, 2137.

Table 4. The Surface-Free Energies, Lifshitz−van der Waals (γ_s^{LW}), the Electron-Acceptor (γ_s^+), and the Electron-Donor (γ_s^-) Parameters of the Cross-Linked HBFP−PEG Coatings Calculated by Three-Liquid Lifshitz−van der Waals Acid−Base (LW-AB) Approach[a]

sample	γ_s (mJ/m^2)	γ_s^{LW} (mJ/ m^2)	γ_s^+ (mJ/ m^2)	γ_s^- (mJ/ m^2)	γ_s^{AB} (mJ/ m^2)
HBFP	22.06	21.98	0.16	0.01	0.08
HBFP−PEG14	23.53	22.87	0.08	1.34	0.65
HBFP−PEG29	27.09	24.68	0.48	2.63	2.25
HBFP−PEG45	31.78	27.88	0.64	5.89	3.89
HBFP−PEG55	36.49	30.87	0.75	10.49	5.62

[a] DM was chosen as the apolar liquid while WT−GL and WT−EG were used as the polar liquid pairs.

was observed previously for block copolymers of poly(ethylene glycol) and polylactide[54] and also for blends of Eudragit RS100 [poly(ethyl acrylate, methyl methacrylate, trimethyl-ammonioethyl methacrylate chloride)] and poly(ethylene glycol).[55] In general, Teflon and other polymers with high contents of perfluoroalkyl groups were shown to exhibit much lower surface energies (6−18 mJ/m^2),[22,56] which have been attributed to the ability of the $-CF_3$ groups to pack densely at the surface. In contrast, HBFP contains only fluoroaryl functionalities. The contribution of the polar interaction parameter (γ_s^p) to the surface energy of HBFP was negligible (0.30 mJ/m^2, ∼1%), reflecting the highly nonpolar nature of the surface. While the γ_s^p values for the cross-linked HBFP−PEG coatings increased in accordance with γ_s, the γ_s^d values did not increase considerably when the PEG content was varied from 0 wt % (HBFP coating) to 14 wt % (HBFP−PEG14) and 29 wt % (HBFP−PEG29). However, when the PEG composition was increased further to 45 and 55%, the γ_s^d values showed an increase of 7 and 14%, respectively. Even though PEG contributes significantly toward γ_s^p as well as γ_s^d (approximately 52 and 48%, respectively),[55] at lower PEG concentrations (0, 14, and 29 wt %), the γ_s^d originates mainly from the HBFP segment, whereas at higher PEG content (45 and 55 wt %), the γ_s^p values vary in accordance with the PEG concentration at the surface, whose surface activity is well-known to be comprised primarily of polar hydrogen-bonding interactions.[54] The observed trend is supported by a similar observation made for poly(ethylene terephthalate) films treated with diamine-terminated PEG.[57]

The surface energies of the HBFP, and the cross-linked HBFP−PEG coatings calculated using three-liquid LW-AB approach (Table 4), were consistent with those obtained from the GM model. The Lewis acid component (γ_s^+) of the solid surface tension of all of the coatings was insignificant (≤0.5 mJ/m^2), owing to the absence of any electron-acceptor groups on the surfaces of these materials. On the other hand, as compared to the pure HBFP coating with a Lewis base component (γ_s^-) value of 0.01 mJ/m^2, the cross-linked HBFP−PEG network with 14 wt % PEG exhibited a γ_s^- value of 1.3 mJ/m^2, which further increased as the PEG wt % was increased to 29, 45, and 55%, respectively (Table 4), which is presumably due to the hydrogen-bonding ability of the ethereal oxygen atoms of the PEG repeat units. On the basis of the total surface energies along with the polar and dispersive components evaluated using the GM model as well as the LW acid−base approach, the majority of interactions at the surfaces

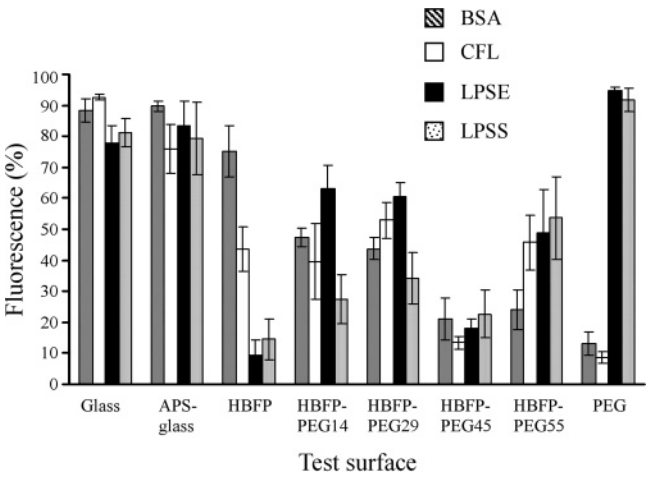

Figure 1. Adsorption of bovine serum albumin (BSA), lectin from *Codium fragile* (CFL), lipopolysaccharide from *E. coli* (LPSE), and lipolysaccharide from *Salmonella minnesota* (LPSS) on the coatings of the cross-linked HBFP−PEG networks was studied by fluorescence microscopy. The HBFP (1b) was used in the preparation of the cross-linked HBFP−PEG materials used in this study. The fraction of surface fluorescing, assumed to be directly proportional to the amount of protein adsorbed, was determined by image analysis following background subtraction and reported as % fluorescence. 100% fluorescence implies that the surface is totally green and 0% means that the surface is totally dark. The HBFP−PEG45 coating, in comparison to other cross-linked HBFP−PEG materials, was the most resistant toward all of the biomacromolecular systems tested.

of the pure HBFP as well as the cross-linked HBFP−PEG network coatings can be construed as van der Waals dispersive while the polar contributions (largely hydrogen bonding) vary in accordance with the PEG content in the network coating. However, the surface energy calculations based on different models are only indicative of the surface properties and caution should be exercised in interpreting these results that are based on the contact angle measurements which, in all probability, do not depend solely upon the surface energetics and other specific interactions such as polymer dissolution/swelling; reorganization also affects the observations, especially in compositionally heterogeneous surfaces. Nevertheless, we believe that the swelling/reorganization of the high-energy PEG component mainly affects the static and the receding contact angles, thus precluding their use in the surface energy calculation, whereas the surface energy values calculated using the advancing contact angles can be considered as a fair measure of the HBFP−PEG surface characteristics.[46]

Adsorption of Biomacromolecules. The behavior of the cross-linked HBFP−PEG coatings toward adsorption of proteins and lipopolysaccharides was investigated by fluorescence microscopy. For this purpose, several biomacromolecules, including proteins (BSA and CFL) and lipopolysaccharides (LPSE and LPSS) conjugated with Alexa Fluor 488 dye, were employed as model systems of varying affinities toward synthetic surfaces, to qualitatively evaluate the ability of the cross-linked HBFP−PEG network coatings to resist biofouling. Analysis of the fluorescence microscopy images allowed for determination of the fraction of the surface fluorescing, which is reported as % fluorescence and interpreted throughout the discussion and also as % surface coverage by the protein or glycoprotein (Figure 1). A 100% fluorescence implies that the surface is completely green and 0% indicates that the surface is totally dark. The dye/protein ratios for BSA and CFL, as determined from UV absorbance of the Alexa Fluor dye at 490 nm with a molar extinction coefficient

(54) Ostuka, H.; Nagasaki, Y.; Kataoka, K. *Sci. Technol. Adv. Mater.* **2000**, *1*, 21.
(55) Lovrecich, M.; Rubessa, F. *Pharm. Dev. Technol.* **1998**, *3*, 123.
(56) Baier, R. E.; Meyer, A. E. *Biofouling* **1992**, *6*, 165.
(57) Kim, K. J. *J. Appl. Polym. Sci.* **1986**, *32*, 6017.

of 71 000 cm^{-1} M^{-1}, were 1.3 and 0.8, respectively, and therefore, fluorescence from the surface was directly correlated to the amount of protein adsorbed to the surface.[58]

As evident from the data presented in Figure 1, complex adsorption profiles were observed for the different biomacromolecules tested upon each of the HBFP and the cross-linked HBFP–PEG surfaces. As compared to the glass and the APS functionalized glass, HBFP and the cross-linked HBFP–PEG surfaces exhibited varying degrees of resistance toward each biomacromolecule employed. The degrees of adsorption of BSA and CFL were higher upon the HBFP coating than the neat PEG surface (Figure 1). BSA possesses higher affinity toward hydrophobic surfaces[59] and, as expected,[60,61] exhibited decreasing affinity toward the surface with increasing hydrophilicity. However, the lowest degree of BSA adsorption was not observed for the most hydrophilic HBFP–PEG55 composite surface, but instead for the HBFP–PEG45 coating. In CFL, even though the degree of adsorption upon the HBFP surface was higher than that on the PEG and the lowest upon the HBFP–PEG45 coating, no clear correlation with the surface hydrophilicity was apparent. The lack of any literature precedence regarding the adsorption patterns of CFL on synthetic surfaces renders the interpretation of these results incomplete. Amphiphilic lipopolysaccharides from *E. coli* (LPSE) and *Salmonella minnesota* (LPSS), having molecular weights of 10 kDa and 3 kDa, respectively, are smaller than BSA or CFL (molecular weights 66 kDa and 61 kDa, respectively) but form micellar aggregates in aqueous solutions and, therefore, are believed to possess affinity toward hydrophilic regions of a surface. It was recently reported[62] that lipopolysaccharides exhibited qualified propensities toward synthetic surfaces and adsorbed preferably to charged hydrophilic surfaces through electrostatic interactions, with little or no adsorption upon hydrophobic surfaces. This behavior is supported by a near 100% surface coverage of LPSE and LPSS achieved on the neat PEG coating and less than 20% surface coverage on HBFP (Figure 1). LPSS follows the expected trend of increasing adhesion with increasing surface hydrophilicity, with the exception of HBFP–PEG45, which is the least fouled of the composite HBFP–PEG surfaces in lipopolysaccharides as well.

Further details about the modes of adsorption of each of the biomacromolecules can be obtained from the fluorescence intensity histograms upon analysis of the fluorescence microscopy images. For BSA and CFL, the number of moles of dye per protein was ~1.0 (0.8 and 1.3, respectively) and, therefore, it was assumed that the fluorescence intensity is directly proportional to the number of protein molecules adsorbed to the surface. Since LPSE and LPSS form micelles in aqueous solutions, the dye/protein ratios were not calculated, and in light of optimal consistency maintained during the experiments, the histograms were interpreted only in terms of relative intensities. The peak position at a higher intensity indicates the presence of the protein or lipopolysaccharide aggregates on the surface. For BSA, peaks at higher intensities with broad distributions were observed (Figure 2) upon the HBFP and the HBFP–PEG14 coatings,

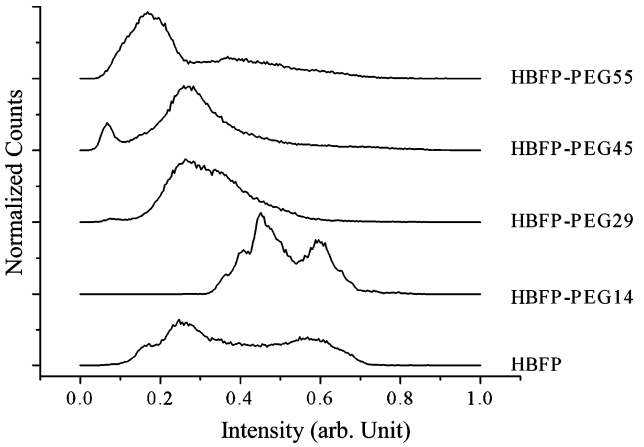

Figure 2. Histograms of fluorescence emission of BSA-AF conjugates from the HBFP, and the cross-linked HBFP–PEG surfaces, obtained using image analysis tools in the MATLAB software. Higher intensity implies aggregation of proteins on the surface. HBFP–PEG45 shows one peak at lower intensity while HBFP–PEG55 exhibits, in addition, a higher intensity peak.

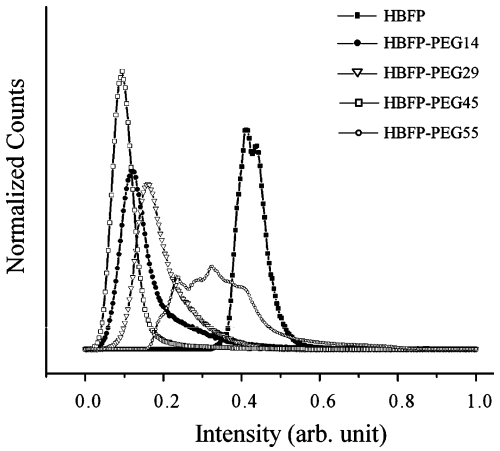

Figure 3. Histograms of the fluorescence emission of the CFL-AF conjugate from the HBFP and the HBFP–PEG cross-linked surfaces, obtained using image analysis tools in the MATLAB software. Higher intensity implies aggregation of the glycoprotein on the surface. HBFP–PEG55 coating exhibited broad higher intensity peaks indicating aggregate formation, while HBFP–PEG45 displayed a single peak at lower intensity.

presumably because of the presence of significant hydrophobic regions leading to higher surface coverage by the protein aggregates in an end-on fashion.[63] At lower surface coverage, on the other hand, the adsorption was almost entirely in a unimolecular side-on direction, resulting in lower intensities as observed for the HBFP–PEG29, HBFP–PEG45, and HBFP–PEG55 coatings (Figure 2).

Even though this model was reported for the adsorption of BSA, it has been suggested that it is applicable to other globular protein–hydrophobic surface systems.[63] Complex intensity distribution profiles were observed for the CFL, LPSE, and LPSS adsorption on the cross-linked HBFP–PEG surfaces, as evident in Figures 3, 4, and 5, respectively. However, the most interesting feature was that the adsorption of all the biomacromolecules tested resulted in low surface coverages with narrow intensity peaks, upon the HBFP–PEG45, in comparison to the most hydrophilic HBFP–PEG55 coating, which encouraged formation of aggregates to a certain extent, as observed by the peaks at higher intensities in the fluorescence emission histo-

(58) Bashir, R.; Gomez, R.; Sarikaya, A.; Ladisch, M. R.; Sturgis, J.; Robinson, J. P. *Biotechnol. Bioeng.* **2001**, *73*, 324.
(59) Sweryda-Krawiec, B.; Devaraj, H.; Jacon, G.; Hickman, J. J. *Langmuir* **2004**, *20*, 2054.
(60) Sharma, S.; Popat, K. C.; Desai, T. A. *Langmuir* **2002**, *33*, 259.
(61) Ying, P.; Gin, G.; Tao, Z. *Colloids Surf., B: Biointerfaces* **2004**, *33*, 259.
(62) Reiter, G.; Siam, M.; Falkenhagen, D.; Gollneritsch, W.; Baurecht, D.; Fringeli, U. P. *Langmuir* **2002**, *18*, 5761.
(63) Xu, T.; Fu, R.; Yan, L. *J. Colloid Interface Sci.* **2003**, *262*, 342.

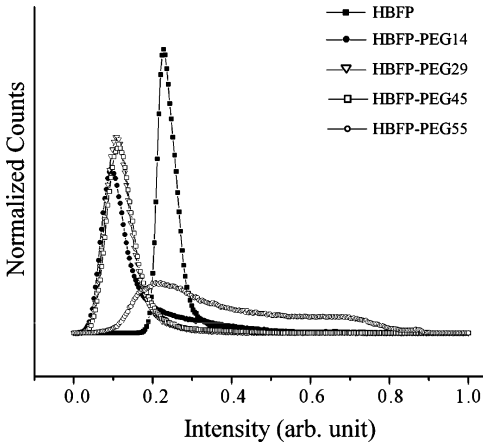

Figure 4. Histograms of the fluorescence emission of the LPSE-AF conjugate from the HBFP and the HBFP−PEG cross-linked surfaces, obtained using image analysis tools in the MATLAB software. Higher intensity implies aggregation of the lipopolysaccharide on the surface. HBFP−PEG55 coating exhibited broad higher intensity peaks indicating aggregate formation, while HBFP−PEG45 displayed a single peak at lower intensity.

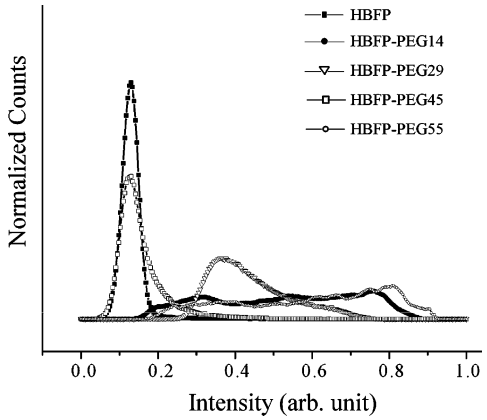

Figure 5. Histograms of the fluorescence emission of the LPSS-AF conjugate from the HBFP and the HBFP−PEG cross-linked surfaces, obtained using image analysis tools in the MATLAB software. Higher intensity implies aggregation of the lipopolysaccharide on the surface. HBFP−PEG55 coating exhibited broad higher intensity peaks indicating aggregate formation, while HBFP−PEG45 displayed a single peak at lower intensity.

grams. Even though several factors such as hydrophobicity,[7,59] protein concentration,[63,64] pH,[64] and surface topography[65] were largely defining the extent to which a protein can adsorb onto a surface, theoretical estimations[66] have predicted that the distance between potential "contact points" for the protein on the surface also plays a significant role. In other words, if the approaching protein is devoid of hospitable "physical space" larger in scale than the protein dimensions on the surface, adsorption can be minimized and reduction in the degree of adsorption is expected to be optimal in the surfaces that exhibit compositional heterogeneities (favorable and unfavorable surface patterns) on length scales similar to those of the protein. With respect to the cross-linked HBFP−PEG surfaces, the HBFP domains can be construed as the hospitable regions for BSA and CFL, while PEG domains are favored by LPSE and LPSS. In HBFP−PEG45, the compositional heterogeneity is believed to result in minimal affinity for different types of proteins or lipopolysaccharides toward the surface. The optimization of this material, relative to other compositions, is supported by investigations of morphologies of the cross-linked HBFP−PEG materials by differential scanning calorimetry. Multiple melting transitions for the HBFP−PEG45 material were explained by the presence of PEG domains that are discrete (giving higher melting transition temperatures), as well as those present as part of smaller domains (exhibiting lower melting transition temperature), in comparison to the HBFP−PEG55 material that exhibited a single melting transition corresponding to larger phase-segregated PEG domains, similar to that of the pure PEG crystallites.[26] In terms of surface energetics, proteins adsorb to nonpolar hydrophobic surfaces via dispersive interactions accompanied by conformational changes on the substrate. On polar hydrophilic surfaces, on the other hand, the extent of polar (electrostatic/H-bonding/Lewis acid−base) interactions between the protein and the surface are presumed to be the factors defining the degree of adsorption.[67,68] In the present study, the experiments were conducted at pH 7.0 which is much greater than the isoelectric points of BSA and CFL (4.0−5.0). At this pH, it can be conveniently assumed that BSA and CFL are fairly basic and therefore are expected to undergo strong interactions with the Lewis acid sites on the surface. From Tables 3 and 4, it is evident that the surface energies of HBFP and the HBFP−PEG cross-linked materials are predominantly composed of dispersive components ($\gamma_s^d \geq 72\%$ and $\gamma_s^{LW} \geq 85\%$). The polar contributions, γ_s^p and γ_s^{AB}, increased from negligible (0.3 and 0.1, respectively) to significant magnitudes (10.0 and 5.6, respectively) as the amount of PEG in the network was increased from 0 to 55 wt %. However, the γ_s^+ and γ_s^- values in Table 4 suggest that the HBFP−PEG coatings exhibit significant Lewis base characteristics at higher PEG contents, which may be resulting in unfavorable polar interactions between the protein and the coatings with 45 and 55 wt % PEG. Therefore, greater BSA adsorption on HBFP, HBFP−PEG14, and HBFP−PEG29 may be construed as a result of strong hydrophobic interactions, while lower degrees of BSA adsorption on HBFP−PEG45 and HBFP−PEG55 may have resulted from unfavorable polar interactions. This rationale may not be applicable in CFL, a glycoprotein, and the lipopolysaccharides because of significant differences in their structures compared to BSA.

Algal Settlement and Adhesion Assays. Zoospore Settlement and Removal. The marine antifouling and fouling-release properties of the cross-linked HBFP−PEG surfaces were investigated by the settlement and release studies of green fouling alga *Ulva* spores and sporelings (young plants formed from the germinating spores). The biofouling assays employing *Ulva* spores were performed upon the HBFP−PEG14, HBFP−PEG29, HBFP−PEG45, and HBFP−PEG55 coatings, whereas the HBFP and PEG surfaces were excluded because of the monolayer coverage by these homopolymers upon the APS-treated glass surfaces and the effects that could result during bioorganism settlement and release for surfaces having very different thicknesses and mechanical properties.[16] The adhesives produced by the spores is a complex glycopro-

(64) Dillman, W. J. J.; Miller, I. F. *J. Colloid Interface Sci.* **1973**, *44*, 221.
(65) Cuppett, C. M.; Doneski, L. J.; Wirth, M. J. *Langmuir* **2000**, *16*, 7279.
(66) Fang, F.; Szleifer, I. *Langmuir* **2002**, *18*, 5497.
(67) Azioune, A.; Chehimi, M. M.; Miksa, B.; Basinska, T.; Slomkowski, S. *Langmuir* **2002**, *18*, 1150.
(68) Manso, M.; Valsesia, A.; Ceccone, G.; Rossi, F. *J. Bioactive Compatible Polym.* **2004**, *19*, 187.

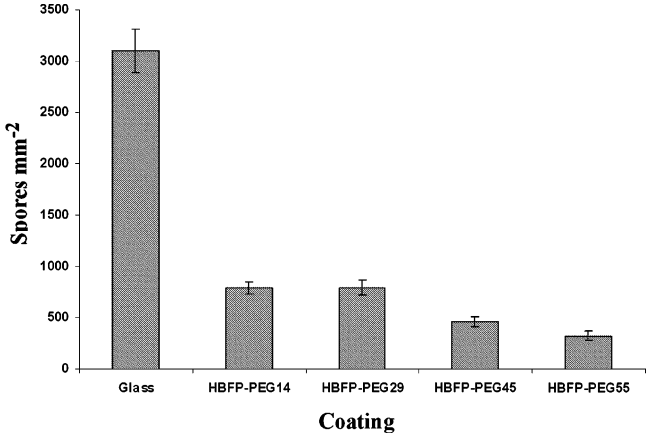

Figure 6. Settlement of green fouling alga *Ulva* (*Enteromorpha)* spores upon each of the cross-linked HBFP–PEG network coatings. The HBFP (1c) was used in the preparation of materials used in these experiments. Mean number of spores attached to the test surfaces after 1 h settlement are shown. Bars represent 95% confidence limits. The spore settlement decreased with increasing hydrophilicity of the surface, and all the cross-linked HBFP–PEG coatings were resistant to the algal settlement compared to the control glass surface, indicating their antifouling behavior.

tein,[6,69] which is very hydrophilic[70] and starts to "cure" as soon as it is released.[30,70] Settlement of *Ulva* zoospores was consistently markedly lower on all the cross-linked HBFP–PEG network formulations compared to acid-washed glass controls (Figure 6). The settlement of spores was lower on surfaces with the highest PEG weight percentages (45% and 55%). One-way analysis of variance followed by Tukey's test indicated significant differences in the data ($F_{4,445} = 432$ $P < 0.05$). Spore density on the cross-linked HBFP–PEG surfaces fell into two groups, HBFP–PEG networks with 45 wt % and 55 wt % PEG, and those with 14 wt % and 29 wt %. The spore densities on surfaces within a particular group were similar but the difference between the two groups was significant supporting the observed trend.

The percentage removal of spores from the cross-linked HBFP–PEG network coatings, upon application of a shear stress of 55 Pa, is shown in Figure 7. Removal from the HBFP–PEG45 coating was significantly different from the rest ($F_{4,445} = 22.7$ $P < 0.05$), which facilitated the removal of approximately 40% of the adhered spores, while 15% or less was removed from the other coatings, including glass.

Sporeling Attachment and Removal. A preliminary experiment was performed with all the test surfaces evaluated with *Ulva* zoospores as well as control PEG and HBFP coatings. The results indicated that removal of 8-day old *Ulva* sporelings was highest from HPFP–PEG45 surface. Hence, the quantitative measurement of growth and removal of sporelings from this surface was directly compared with a PDMSE standard, T2 Silastic, which exhibits good fouling-release properties with respect to macrofouling organisms.[71] *Ulva* sporeling growth upon the HBFP–PEG45 coatings was patchy compared to that on glass and PDMSE, the former being due to detachment of some very weakly adhered sporelings when the growth medium was replenished. The significantly lower biomass

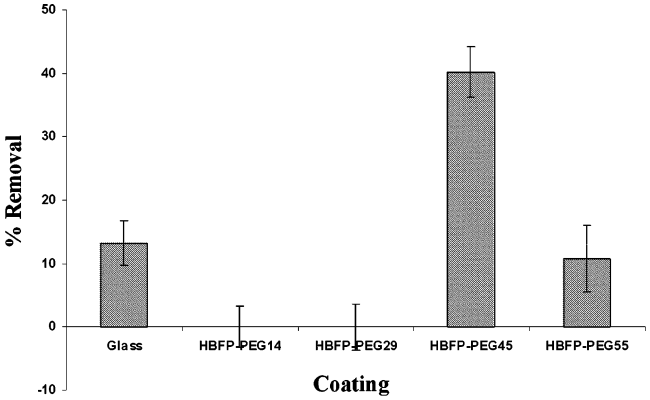

Figure 7. Percentage removal of attached *Ulva* zoospores from the cross-linked HBFP–PEG coatings, after 1 h settlement following exposure at 55 Pa wall shear stress in a flow channel. Bars represent 95% confidence limits from arc-sine transformed data. The removal was the greatest from the coating with 45 wt % PEG, indicating its unique potential fouling-release properties.

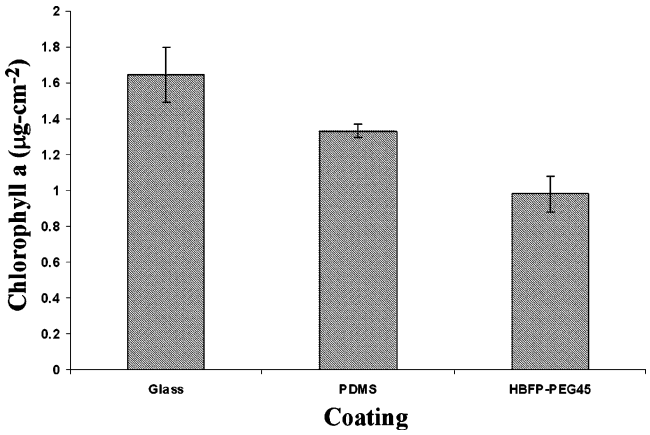

Figure 8. Biomass of *Ulva* sporelings after 8 days growth on glass, PDMSE, and the HBFP–PEG45 coatings. Biomass was measured as chlorophyll$_a$. The means of four replicates ± standard error are shown. The lower amount of biomass on the HBFP–PEG with 45 wt % PEG coating is due to loss of weakly adhered sporelings when the growth medium was changed.

associated with the HBFP–PEG45 surface compared to glass ($F_{2,9} = 4.76$ $P < 0.05$) after 8 days of growth reflects this loss (Figure 8) and suggests that the surface was very inhospitable for growth. Removal of sporelings was significantly different from all the three surfaces tested ($F_{2,9} = 110.9$ $P < 0.05$). Greatest removal was from the HBFP–PEG45 surface with a mean detachment of over 90% (Figure 9), which was approximately twice from that of the fouling-release PDMSE surface.

All of the cross-linked HBFP–PEG surfaces were relatively hydrophobic compared to glass and, in general, spore settlement increases with decreasing wettability.[72] However, the relationship does not hold true for all surfaces and the strength of attachment of spores, and sporelings do not show a direct correlation with surface wettability, although in common with most other macrofouling organisms,[3,23] lower adhesion strengths of spores and sporelings are found on fouling-release coatings based on PDMS.[34,73] Interestingly, it has been shown that while the settlement of zoospores decreases with increasing

(69) Callow, J. A.; Crawford, S. A.; Higgins, M. J.; Mulvaney, P.; Wetherbee, R. *Planta* **2000**, *211*, 641.
(70) Finlay, J. A.; Callow, M. E.; Schultz, M. P.; Swain, G. W.; Callow, J. A. *Biofouling* **2002**, *18*, 251.
(71) Sun, Y.; Guo, S.; Walker, G. C.; Kavanagh, C. J.; Swain, G. W. *Biofouling* **2004**, *20*, 279–289.
(72) Ista, L. K.; Callow, M. E.; Finlay, J. A.; Coleman, S. E.; Nolasco, A. C.; Simons, R. H.; Callow, J. A. *Appl. Environ. Microbiol.* **2004**, *70*, 4151.
(73) Schultz, M. P.; Finlay, J. A.; Callow, M. E.; Callow, J. A. *Biofouling* **2000**, *15*, 143.

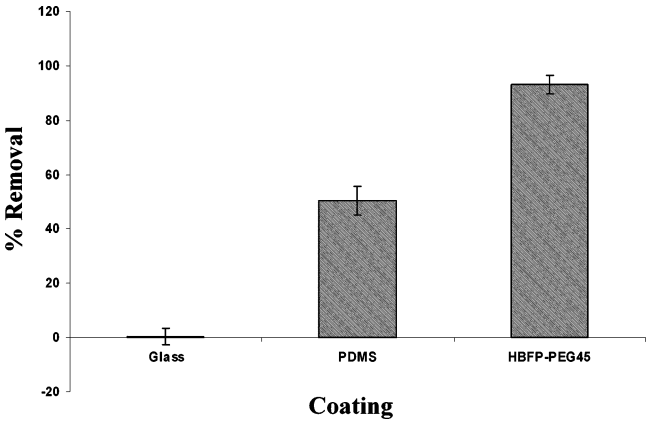

Figure 9. Percentage removal of biomass following exposure to 55 Pa wall shear stress. The means of four replicates ± standard error are shown. The cross-linked HBFP−PEG coating with 45 wt % PEG was more effective in fouling release than the standard PDMS coating.

wettability, the strength of attachment is typically greater on the hydrophilic surfaces.[15] Therefore, the trend observed in the settlement of spores upon the cross-linked HBFP−PEG surfaces (Figure 6) was not surprising and the lower settlement of spores upon HBFP−PEG55/HBFP−PEG45 coatings compared to the HBFP−PEG14 and HBFP−PEG29 surfaces could be explained in terms of the greater hydrophilicity of the former. The surface compositional heterogeneity attributed to the lowest degree of protein and lipopolysaccharide fouling upon the HBFP−PEG45 coating can also be expected to define the best marine antifouling properties observed for this coating. The observation that sporelings released much more effectively from the HBFP−PEG45 surface than the PDMSE (Figure 9) is therefore especially interesting and suggests that this nanostructured material has promising properties in the practical control of soft fouling. The main properties that are now accepted as being of utmost importance for the release of hard foulers, for example, barnacles, from PDMSE are surface energy, bulk modulus, and coating thickness.[74] The release of soft fouling from PDMSE is less clearly correlated than that for the hard foulers although recent data indicates a role of all three parameters (unpublished work).

Conclusions

The complex surface topographies, morphologies, and compositions of nanoscopic dimension exhibited by coatings based on amphiphilic cross-linked networks of hyperbranched fluoropolymer (HBFP) and poly(ethylene glycol) (PEG) with PEG weight percentages of 14, 29, 45, and 55%, and prepared on 3-aminopropyltriethoxysilane functionalized microscope glass slides, provided for enhanced ability to inhibit protein adsorption and marine organism settlement. The polar and dispersion components of the surface-free energies of the HBFP and the cross-linked HBFP−PEG coatings were evaluated using geometric-mean and Lifshitz−van der Waals acid−base approaches. The total surface-free energies increased with increasing PEG content in the cross-linked network because of segregation of PEG to the polymer−water interface upon contact with water. The cross-linked HBFP−PEG coatings were resistant toward the adsorption of bovine serum albumin, a lectin, and lipopolysaccharides (from *E.coli* and *Salmonella minnesota*) in comparison to the control surfaces, as manifested in the fluorescence microscopy investigations, which revealed complex interaction profiles for each of the biomacromolecules upon the surfaces with varying wettabilities. Either of the pure HBFP, with the lowest surface energy, or the PEG coating, well-known for its optimal protein resistance, was ineffective in preventing fouling by all the biomacromolecules with varying affinities toward hydrophobic and hydrophilic surfaces. On the other hand, the HBFP−PEG45 coating, in comparison to the most hydrophilic HBFP−PEG55 or any other coating examined, was the most effective in preventing protein and lipopolysaccharide adsorption and *Ulva* zoospore settlement as well as facilitating zoospore release, suggesting its high potential applicability as efficient nontoxic marine antifouling and fouling-release coating. Furthermore, this observation underscores the validity of our hypothesis that the compositional and morphological heterogeneity is the key to achieving surfaces that can prevent biofouling.

Acknowledgment. This material is based upon work supported by contracts from the Office of Naval Research (N00014-02-1-0326 to KW; N00014-02-1-0521 to J.A.C. and M.E.C.), which are gratefully acknowledged. The authors would like to thank Mr. Debashish Pal for providing support in generating the fluorescence microscopy image histograms using MATLAB software and Professor A B Brennan, University of Florida, for providing slides coated with T2 Silastic.

LA048015O

(74) Berglin, M.; Lonn, N.; Gatenhohm, P. *Biofouling* **2003**, *19*, 63.